Pharmaceutical Sciences, 2020, 26(4), 406-413
doi:10.34172/PS.2020.36
https://ps.tbzmed.ac.ir/

Research Article

Molecular Dynamics Simulation, Characterization and *In Vitro* Drug Release of Isoniazid Loaded Poly-ε-caprolactone Magnetite Nanocomposite

Aram-Dokht Khatibi[1*], Zarrin Es'haghi[2], Hamid Mosaddeghi[2], Davoud Balarak[1]

[1] *Department of Environmental Health, School of Public Health. Zahedan University of Medical Sciences, Zahedan, Iran.*
[2]*Department of Chemistry, Payame Noor University, 19395-4697 Tehran, Iran.*

Article Info

Article History:
Received: 17 February 2020
Accepted: 4 May 2020
ePublished: 25 December 2020

Keywords:
-Drug delivery
-Magnetite nanoparticles
-Poly-ε-caprolactone
-Isoniazid
-Tuberculosis
-Molecular dynamics simulation

Abstract

Background: This study reports on the development of a controlled-release isoniazid (INH) drug delivery system using poly-ε-caprolactone (PCL) functionalized magnetite-nanoparticles (MNPs), as a theoretical potential tool for tuberculosis (TB) chemotherapy.

Method: The magnetite Fe_3O_4 core was fabricated by the co-precipitation method and coated with PCL by emulsion polymerization. INH was loaded onto the PCL-MNP surface to shape an INH-PCL-MNP nanocomposite. Deposing the INH on the nanocomposite surface was demonstrated through the molecular dynamics simulations. To investigate the stability of the polymer, the root-mean-square deviation (RMSD) and the radius of gyration (Rg) were calculated. The composite was characterized by Scanning electron microscopy (SEM) and X-Ray diffraction (XRD) and Fourier transform infrared spectroscopy (FTIR). Mycobacterium tuberculosis was used to assess the antimicrobial activity of the nanoparticles. The drug loading efficiency, drug content, and in-vitro release behavior of the INH-PCL-MNPs were evaluated by UV–Vis spectrophotometry.

Results: RMSD of PCL show that the structure of polymer after 40 ns is stable. INH molecules interested to spend more time close to the polymer. Rg of PCL indicated that PCL folded and radius of gyration changed near 1nm. The drug loading efficiency and drug content of the NPs were 720±46 mg/g and 69.3±3.8 (%), respectively. The compound showed a strong level of activity *in-vitro*. The amount of drug release at all times was above the minimum inhibitory concentration (MIC) (6 µg/ml).

Conclusion: INH-PCL-MNP nanocomposite have been effectively used as a potential tool to treat TB infections and a magnetic drug carrier system.

Introduction

Mycobacterium tuberculosis (MTB) has infected nearly one-third of the world's population, developed in approximately eight million new cases, and led to two million deaths each year.[1] Isoniazid (INH) is an antimycobacterial agent applied widely as first-line therapy of tuberculosis and is defined by a short half-life ranging from 1 h to 4 h which mostly relies on the metabolic rate.[2] MTB is conventionally treated by regular administration of many drugs for 6 months or more.[3] Considering the poisonous side effects of pills, degradation of drugs before reaching their target tissue, low penetrance, and Patient disrespect, the clinical management of this disease is quite limited. Due to these drawbacks, the conventional chemotherapy methods should be modified in a way that the delivery or carrier system be developed to release drugs gently over long times.[4,5]

In the last decade, different carrier systems, like liposomes and nanoparticles, have been studied to manage a variety of clinical conditions in a better way.[6,7] Nanoparticles as carrier systems have great potential for treating tuberculosis (TB).[8,9] Their high carrier capacity, great stability, and feasibility of variable ways of administration, including oral application and inhalation, which can be mentioned as the most significant scientific benefits of nanoparticles used as drug carriers.[10,11] Moreover, nanoparticles can be planned to create a sustained drug release. Such things allow the enhancement of drug bioavailability and reduction of the dosing frequency.[12] These systems, if successfully developed, may have the advantage of promoting the control of the drug blood levels.[13] This, in turn, can enhance efficacy by improving patient compliance, and extending and maintaining drug blood levels for an extended period

*Corresponding Author: Aram-Dokht Khatibi, E-mail: khatibi.aram@gmail.com

which are all required for effective treatment.[14]

Polymeric carrier systems help to reduce side effects and enhance efficacy and are more helpful compared to the injection method and controllable dose and rate.[15,16] Poly-ϵ-caprolactone (PCL), is a biodegradable and synthetic biocompatible polymer, which is widely investigated for controlled drug delivery applications in numerous studies.[17]

Magnetite nanoparticles (MNP) are a prevalent type of magnetic materials that are common in use. Given their super-paramagnetic traits, high specific area, and a wide choice of surface functionalization, magnetic particles can interact with many biological molecules in various ways.[18] Focusing on the separation process, these particles may separate the target bio-molecules with a single magnet instead of centrifugation or precipitation.

Moreover, because of the magnetic properties of these nanoparticles, one can easily envision their magnetic field direction to fight undesirable micro-organisms existence on demand. The chemical stability and possible chemical adaptation by coating the iron oxide cores with several kinds of layers (e.g., silica, gold, and polymers) can be regarded as desirable properties attributed to iron oxide nanoparticles and they are considered as the individual kind of MNPs that have been accepted by the FDA for medical applications.[19,20]

The current research aimed to improve a magnetite poly-ϵ-caprolactone-functionalized nanoparticulate (PCL-MNP) system for drug delivery that could carry and release the drugs over long times. INH is regarded as one of the most important drugs which are widely used in the treatment programs for TB. The potential anti-TB activity of INH is measured by minimum inhibitory concentrations (MIC) using broth microdilution and used to illustrate the effectiveness of the proposed method.

Since biocompatible PCL plays the major role in the INH loading, and on the other hand, the polymer had to be laid on a nanostructured biocompatible base therefore, it was preferred to use the Fe_3O_4 as a biocompatible and bio safe to the human base material.

The main goals of the present study were to entrap INH within biodegradable PCL-MNP by emulsion polymerization method and characterization of drug content of the system, surface morphology, and in vitro drug release studies. Since the position of INH-PCL-MNPs is controllable by a magnetic field, this method offers significantly more theoretical potential for developing theranostic tools for microbial infections.

On the other hand, interfacial interaction between drug and PCL-functionalized nano-particulate and the molecular structure of them can be identified as key parameters for the binding properties and the resulting drug delivery process. These details are usually difficult to address using experimental methods. Here, molecular dynamics (MD) simulations were used to examine the delivery mechanism of INH models and chemically modified nanocomposite surfaces in-vitro release process. This highlights the reputation of molecular structure details to molecular adhesion.

Materials and Methods

Materials

All materials were the highest purity available. Isoniazid gave from Daroopakhsh Pharmaceuticals, Tehran, Iran. Ferric chloride ($FeCl_3.6H_2O$), ferrous chloride ($FeCl_2.4H_2O$), and sodium hydroxide (NaOH) (Merck, Darmstadt, Germany) were used to nanomagnetite preparation. All solvents were HPLC grade and obtained from Merck. Phosphate buffered saline (PBS) pH 7.4, poly- ϵ-caprolactone (PCL), polyvinyl alcohol (PVA), and middle brook 7H9 broth base were obtained from Sigma-Aldrich (St. Louis, MO, USA). A milli-Q system (Millipore, USA) was used to prepare ultra-pure water.

Apparatus

Fourier transform infrared spectra (FTIR) of coated MNPs were recorded on a (M-500 Fast-Scan IR Spectrometer Buck Scientific, East Norwalk, CT 06855, United States) and scanning electron microscopy (SEM) (KYKY EM3200 scanning electron microscope) was used for investigation of nanoparticle microstructure. Centrifuge (f) and ultrasonic bath (Elmasonic D-7822, Germany) were used to prepare maps. A Shimadzu-2100 (Japan) double-beam UV–Vis spectrophotometer with a 1 cm quartz cell was applied for INH release studies.

Preparation of magnetite nanoparticles (MNPs)

The magnetite Fe_3O_4 core of this Nano-sorbent was fabricated by co-precipitation of ferrous (Fe II) and ferric (Fe III) aqueous solution in the presence of ammonium hydroxide. In this way, 2.0 g $FeCl_2$ and 5.2 g $FeCl_3$ were put in 25 mL ultra-pure water (in the molar ratio of 2:1) in a flask. The agitation of the solution was performed using a magnetic stirrer. Then, the solution was deoxygenated by Argon for about 30 minutes. Following this, about 250 mL alkaline solution of 1.5 M NaOH was added to the solution (drop by drop). The resultant black powder was washed three times using double distilled water and it was separated from the solution by a simple magnet.[21,22]

Formulation of INH loading PCL functionalized magnetic nanoparticles (INH-PCL-MNP s)

The INH-PCL-MNPs was prepared by applying an emulsion solvent extraction/evaporation technique.[23] The experimental parameters impacting the performance of INH-PCL-MNPs preparation were investigated. Briefly, a mixture of 500 mg of water dispersed magnetite nanoparticles and INH (100 mg) was added to a solution of 10.0 mL dichloromethane and 300 mg of PCL while stirring was performed in the ultrasonic bath for 5 minutes (23.6 Np speed) then 100 mL of 2 % PVA was added to form w/o/w emulsion. The magnetite and PCL emulsion were shaken quietly at 200 rpm at 20° in 50 mL of distilled water for 3 hours until the evaporation of dichloromethane.

After that, the resultant material was washed with double distilled water three times before magnetically separation and drying. Drug-free PCL-MNP was prepared by substituting normal saline for the INH.

Characterization of nanocomposites

Molecular Dynamics (MD) Simulations

In the current study, *MD* simulations were conducted by GROMACS ver. 5.0.4,[24] with the Amber ff99SB force field[25] for the simulation of PCL and INH. Charges on all atoms were measured with the Restrained Electrostatic Potential (RESP) approach,[26] by applying electrostatic potentials assessed at the HF/6-31G* theory level and sampled with the Merz-Kollman scheme.[26] The parameterization of INH as a drug was generated by the Acpype code.[27] The initial structure of PCL with 41 monomers and six molecules of INH in various directions concerning the polymer used in this work are shown in Figure 1.

To investigate the stability of the polymer, the root-mean-square deviation (RMSD) and the radius of gyration (Rg) were estimated that are shown in Figure 2. RMSD is the measure of the average distance between the atoms and stability of the system during simulation. Rg is the measure of structure compactness.

In continue, the dynamic behavior of drug molecules near the polymer surface was mainly studied. For this purpose, the minimum distance between INH molecule and PCL was calculated, the results of which are shown in Figure 3.

Surface functionalization confirmation

Surface changes in MNPs, PCL-MNPs, and INH-PCL-MNPs were studied using FTIR spectroscopy at $4cm^{-1}$ resolution in the wave number range of 4,000 to 400. The FTIR spectra of INH were recorded for comparison. The results are shown in Figure 4.

Morphology

Scanning Electron Microscopy (SEM) operating at 100 kV was used to investigate the morphology of PCL-MNPs.

Calculation of drug loading and encapsulation efficiency

The quantity of INH captured inside PCL-MNP was measured by considering the quantity of drug in the aqueous solution recovered after the particles' magnetic separation.[28] INH was analyzed by spectrophotometric method (263 nm).[29] The drug encapsulation efficiency was stated as the percentage of drug entrapped concerning the theoretical value and drug loading stated as the amount of drug entrapped per gram of nanosorbent.[14] The calibration curve was plotted against the concentration levels of the INH in PBS pH 7.4. Each step was repeated 5 times. The calibration curve of INH showed linearity and was a wide range of 0.001-30.0 µg/ml concluded a correlation coefficient of 0.9988 with the equation Y=0.0433X-0.0078. The INH-PCL-MNP s (10 mg) were dissolved in 10 ml aqueous solution of PBS under sonication for 20 min. Nanoparticles were simply separated with a permanent magnet and the amount of INH was measured in the solution. The earliest UV studies have indicated that the existence of dissolved polymers did not interfere with the drug absorbance at 263 nm.

Determination of nanocomposite minimum inhibitory concentration (MIC)

Test compound (PCL magnetite nanoparticles containing entrapped INH) was assessed for in-vitro anti-mycobacterium activity. The MIC was investigated for M. tuberculosis $H_{37}Rv$, at the technique of the accepted micro-dilution reference technique of antimicrobial susceptibility testing.[24] The MIC was determined over a range of 1.0–512 µg/ml. MTB $H_{37}Rv$ strain was applied in Middle brook 7H-9 broth which smeared with the INH as standard and nanocomposite as test material and incubated at 37°C for 4 weeks. The bottles were checked for growing two times a week for 3 weeks. Readings were done on the last day of the fourth week. The presence with a turbidity of 1×10^6 CFU/ml was measured as bacterial growth and indicated stability to the nanocomposite. Confirmation of the growth was performed by making a smear from each bottle. The nanocomposite was compared with the INH (MIC=0.25 µg/ml).[30] All experiments were performed three times.

In-vitro release studies

INH-PCL-MNPs and empty PCL coated magnetite nanoparticles (PCL-MNPs) as control material was synthesized as termed earlier. They dumped in 5 ml of PBS kept in a 37°C incubator. every day for 7 days and then weekly up to 6±8 weeks, after magnetic separation of the suspension, the supernatant collected to find the drug release amount.

The drug release concentration in the supernatant was done by the spectrophotometric analyzer. The outcomes were stated as INH concentration released in the solution of buffer at various time intervals.

Results and Discussion

Details of molecular dynamics simulations

This system (included PCL and INH molecules) was located in the center of a box and about 1.0 nm from the edges and then solvated in 16470 TIP3P water model molecules. The system's pH was set ~7. The energy of the system was decreased by using a short steepest descent minimization algorithm (while the polymer and drug molecules were saved in their primary conformation). Afterward, this system ran under 1nano second (ns) with constant Number, Volume and Temperature (NVT)[31] and constant Number, Pressure and Temperature (NPT)[32] canonical ensembles to get a suitable temperature (300°K) and pressure (1 bar). The particle mesh Ewald (PME) method was used to calculate the long-range electrostatic interactions with an assigned interpolation order of 4.[33] For short-range Van der Waals and short-range electrostatic interactions used 1.4 nm cutoff and the LINKS algorithm[34] for covalent bond constraints were utilized. For MD run,

two 100 ns consecutive MD runs were performed on the whole system. All results averaged on 200 ns. The final configuration of INH molecules near PCL is shown in Figure 1. INH molecules near PCL had more tendency to be located so that the aromatic ring of INH molecule was parallel to the polymer surface.

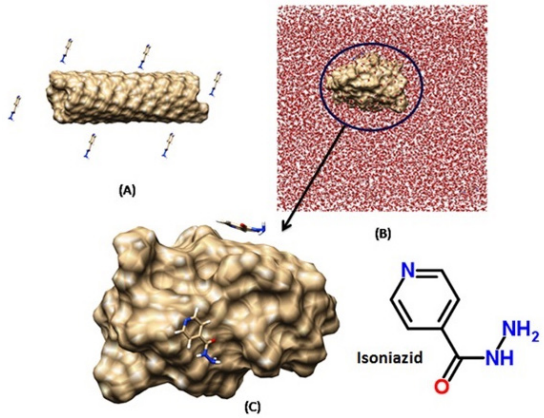

Figure 1. (A) An initial configuration of polymer and drug, (B) simulation box (C) and final configuration of polymer and drug after 100 ns.

The RMSD and the Rg were estimated. These results indicated that the polymer folded during this time and got a stable structure. In fig 2, RMSD of PCL show that the structure of polymer after 40 ns (40000ps) is stable. Rg of PCL indicated that PCL polymer folded and Rg changed near 1nm.

The dynamic behavior of drug molecules near the polymer surface was averaged over all six INH molecules. The results showed that INH molecules interested to spend more time close to the polymer. The favorable distance was 2Å from the polymer surface.

Then, the hydrogen bond lifetime and several hydrogen bonds in this system were assessed. The results showed that the average lifetime of hydrogen bonds in this system (between PCL and INH molecules) was 6.7 ps and also the average number of hydrogen bonds was 0.2. As known, the INH molecule could form two hydrogen bonds with PCL. It seemed that the folded structure of the polymer and geometrical position of INH did not allow to create more hydrogen bonds. The results showed that the hydrogen bond network in this system was not so strong; however, it had the benefit for transfer INH as the drug, because the drug release can be easily done in the target cell.

The Fourier transform infrared spectroscopy (FTIR) analysis

The FTIR measurements confirmed the encapsulation of magnetite with PCL. The FTIR outcomes were presented in Figure 4 (a) FTIR spectra of MNPs and (b) PCL microencapsulated nanomagnetites. As can be indicated, the carbon-oxygen stretching bonds in the area of 700 cm^{-1} to 1500cm^{-1} were from PCL composites; carbonyl band, C=O, at 1718cm^{-1} symmetric and asymmetric of CH_2, at

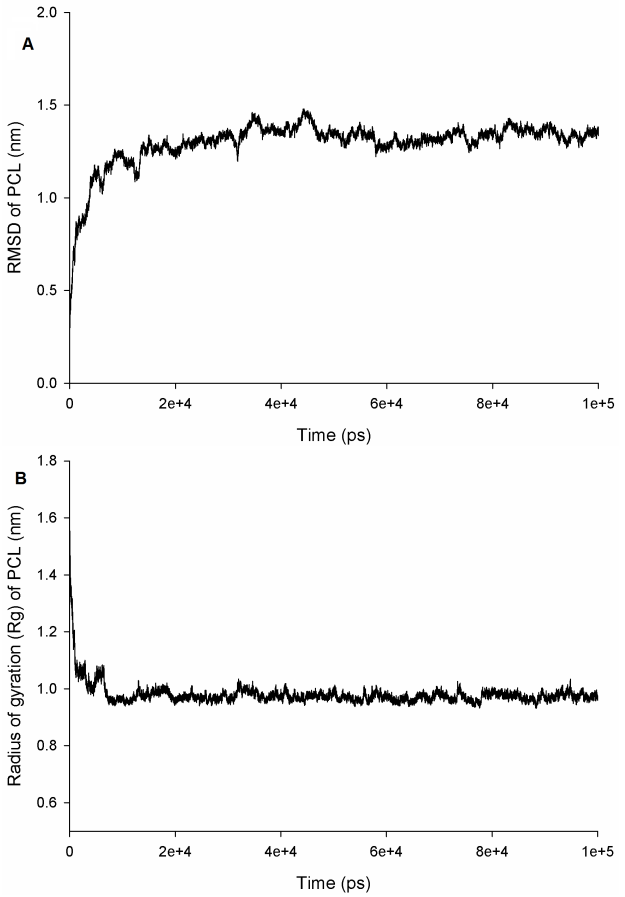

Figure 2. (A) The root-mean-square deviation (RMSD) and (B) the radius of gyration (Rg) for PCL.

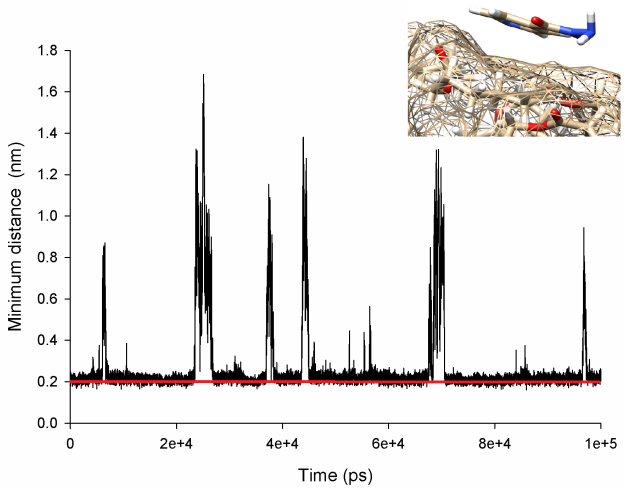

Figure 3. The minimum distance between PCL and isoniazid molecules.

2923 cm^{-1} and 2941 cm^{-1} were also related to the PCL.

In Figure 4 (c), the FTIR spectrum of INH was shown. The 1551 cm^{-1} strong bond was related to ring N=C symmetric stretching vibrations. The band at 1334 cm^{-1} might be because of vibrations of C-N stretching. A very strong band at 1669 cm^{-1} was related to C = O stretching vibrations. The band appearing at3300 cm^{-1} was attributed to N-H stretching vibration. The bands at 682 and 1430 cm^{-1} were

assigned to C-C=O and H-N-N bending, separately.[35] Figure 4(d) showed the FTIR spectrum of INH-PCL-MNPs. As can be seen, the band at 3200 cm^{-1} was owing to N-H stretching vibration and a very strong band appearing at 1556 cm^{-1} was assigned to ring N-C symmetric and the band at 1634 was related to C = O stretching vibrations and they came from the INH. This result proved the existence of isoniazid in nanoparticles.

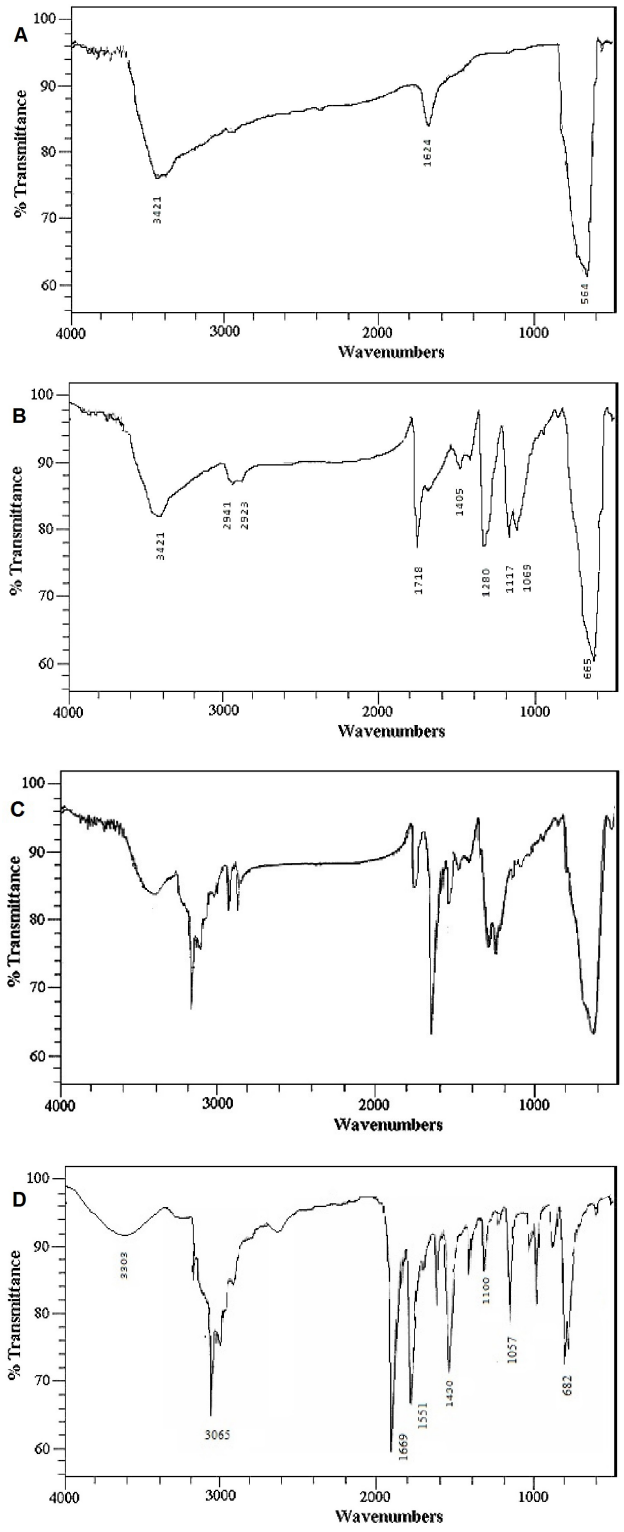

Figure 4. (A) The FT-IR spectrum of (B) nanomagnetites (MNP) s, b) the polycaprolactone coated nanomagnetites (PCL-MNP) s, (C) Isoniazid (INH), and (D) Isoniazid loaded polycaprolactone coated nanomagnetits (INH-PCL-MNPs).

Scanning electron microscopy (SEM) and X-Ray diffraction(XRD)

SEMmethod was performed to check the morphology of nanoparticles. In these cases, the particle size was around 50 nm and almost sphere-shaped and they had smooth and uniform surfaces. The SEM of nanoparticles was shown in Figure 5.

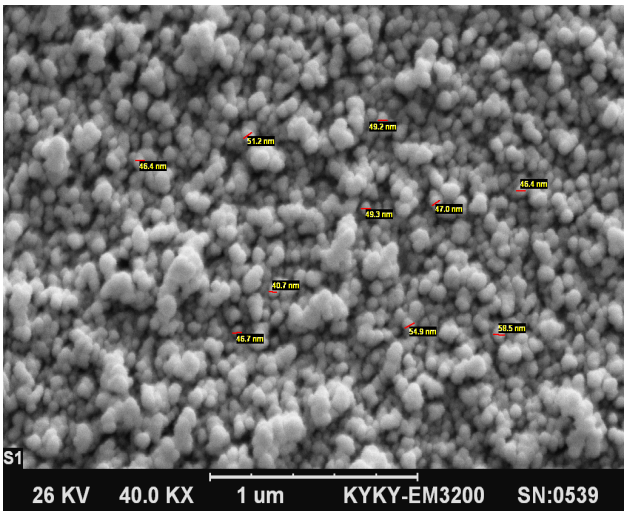

Figure 5. The SEM image of the synthesized nanocomposite.

Figure 6 shows the XRD pattern of Fe_3O_4 nanoparticles. The graph indicates specific peaks at 2 θ values of 31, 36, 43, 54, 57 and 63, related to phases 220, 311, 400, 442, 440, and 550 of Fe3O4 nanoparticles, respectively. So, it can be decided that Fe_3O_4 nanoparticles have been successfully fabricated.

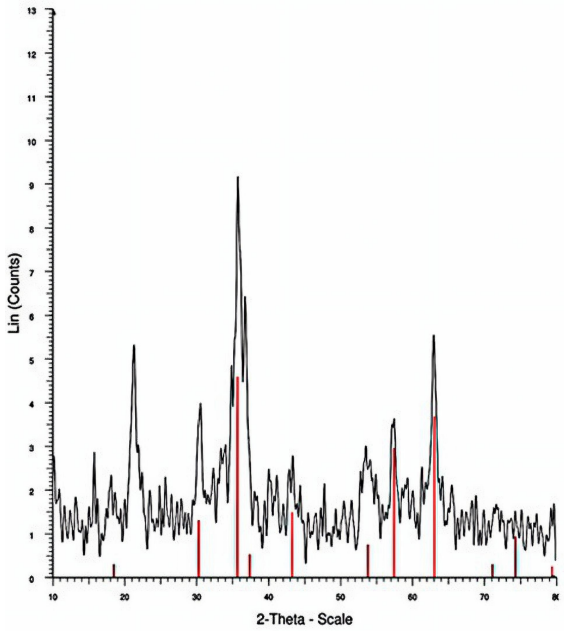

Figure 6. The X-ray diffraction patterns of Fe_3O_4 nanoparticles.

Optimizing the INH loaded PCL coated magnetite nanoparticles (INH-PCLMNPs) preparation conditions

Optimizing the phase ratio (organic/aqueous phase) concerning the drug entrapment percent

Phase ratio was optimized regarding drug entrapment efficiency percent and other parameters were kept constant (drug/sorbent ratio: 1:2, PVA in water 2%, sonication time 5 min). To optimize, the ratio of organic phase to the aqueous phase from1:1 to 1:20 (v/v) and the percent of the drug entrapment was investigated. Increases in the drug entrapment percent were observed when 1:10 of phase ratio was used. With increasing phase ratio from 1:10 to 1:20 (v/v), a decrease in the drug entrapment percent was recorded. This decrease can be a result of forming some aggregates in the formulation. The phase ratio amount of 1:10 was considered for further experiments.

Optimizing the surfactant concentration concerning the drug entrapment percent

an aqueous PVA solution was used as a surfactant in preparing microspheres, %) For this purpose various PVA concentrations (0.5 to 3.5%) were reviewed (drug/sorbent ratio: 1:2, phase ratio: 1:10, sonication time 5 min). The results showed that 2% of the aqueous PVA solution was sufficient for satisfactory results. After this point, there were no changes in the drug entrapment efficiency.

Optimizing the drug/polymer ratio concerning the drug entrapment percent

To optimize the drug/polymer ratio, several ratios of drug and PCL (1:1, 1:2, 1:3, and 1:5 w/w) were examined and a fixed amount of PVA in water 2%, phase ratio:1:10, sonication time 5 min were considered. The drug entrapment efficiency percent was determined. As the result demonstrated, the drug entrapment efficiency percent generally increased with the drug/polymer ratio of 1:3 and for a ratio of more than 1:3, a reduction was detected in the extraction efficiency. This decrease was maybe because of the increased viscosity and might result in the low dispersibility of PCL-MNPs in the solution. Therefore, the drug/polymer ratio of 1:3 was fixed.

Optimizing the sonication time concerning the drug entrapment percent

To investigate the effect of sonication time on drug entrapment percent, different sonication times, i.e., 1, 5, 10, 15, and 20 minutes were studied. The percent of the drug entrapment was determined and recorded. According to the results, an increase in the drug entrapment percent was observed by increasing contact time up to 5 min. The additional increase in contact time did not end in an important increase in the drug entrapment percent. That is why, in our research, the sonication time of 5 min was preferred.

Determining the drug loading and entrapment efficiency

The drug encapsulation efficiency was stated as the fraction of drug captured concerning the theoretical value and the drug loading stated as the quantity of INH captured per gram of nano sorbent in various drug/ adsorbent ratio. As a result, the best drug encapsulation was 69.3%, whereas drug loading was 720 mg drug per gram of nanosorbent (See Table 1). Losing the drug in the emulsion solvent extraction/evaporation method was only accounted for the washing processes. In this study, the magnetic separation was applied and there was no need for a filtration process that could lead to losing the drug. The effect of the drug/polymer ratio on drug loading and entrapment efficiency was investigated. The drug/polymer ratio of 1:3 leads to the maximum concentration of INH entrapped in the sorbent and loading of it into the medium. A decrease in the results was detected with a comparative rise in the amount of PCL-coated adsorbent. This can be due to the increase in the density of the polymer context with increasing polymer concentration (1:5).[29] Though, the drug/polymer ratio under 1:3 presented low entrapment efficiency (Table 1) owing to the low amount of the sorbent.

Anti-tubercular activity

The anti-mycobacterium activity of the nanocomposite was checked against M. tuberculosis $H_{37}Rv$ at 512, 256, 128, 64, 32, 16, 8, 4, 2, and 1 µg/ml. The nanocomposite showed inhibition at concentration 6 µg/ml. This provided good evidence of the anti-TB activity of the coated nanoparticles. It is highly suggested that future researches contain an in vivo analysis and determine the stability of these novel nanocomposites.

Drug release studies from PCL-MNPs

The concentration of INH released PCL-MNPs demonstrated an initial (up to 24 h) burst release and a sustained-release of up to 6 days followed by a negligible release of the drug up to 4 weeks. Much more release was observed by particles containing more drugs. The burst release in the first 24 h was ascribed to the INH release from the surface of the PCL-MNPs. The next stage

Table 1. The fabrication and characteristics of PCL-MNPs with INH.

	Formulation			
Drug: Polymer ratio	A1 1:1	A2 1:2	A3 1:3	A4 1:5
Entrapment efficiency (%)	41 ± 4.3	48.6 ± 3.7	69.3 ± 3.8	65.4 ± 4.2
Drug loading mg/g nanosorbent	685 ± 26	711 ± 43	720 ± 46	716 ± 22

Results are mean ± SD of 3 replications

involving sustained release was related to the drug release from the inside of the nanoparticles (Figure.7). It should be noted that the amount of drug release at all times was above the MIC (6µg/ml). As expected, empty PCL-MNPS did not show any release of INH. All the experiments were repeated 3 times for each test and the results were presented as mean ± SD and verified using the analysis of variance (P>0.05).

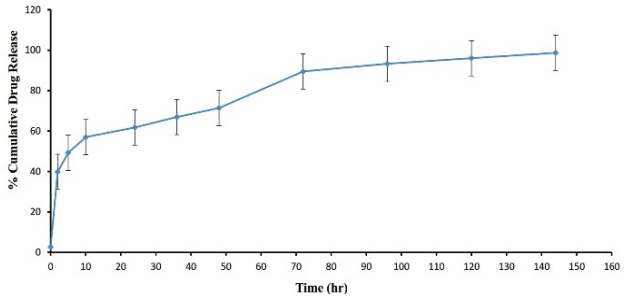

Figure 7. *In vitro* Cumulative drug release profile of INH loaded PCL-MNP, up to 6 days (144 hr). Data represent mean±SD, n: 3.

Conclusion

Magnetite nanoparticles microencapsulated with PCL microspheres have been effectively fabricated and used as a potential tool to treat tuberculosis infections and used as a magnetic drug carrier system. The polymer layer on the nanoparticles creates a spherical shape and also disperses and enhances the effective surface area of the particles. So offered suitable nanosorbent and nanoparticulate drug carrier system. The magnetic core enables the nanoparticles to be rapidly separated from the environment by the magnet the current study, INH loaded PCL-MNP as a therapeutic approach towards tuberculosis fabricated and characterized. INH loaded PCL-MNP was organized by the emulsion solvent extraction/evaporation technique for prolonged release. The drug/adsorbent ratio was considered. The good entrapment efficiency (69.3%) was gained using this technique. The drug loading from the nanosorbent was720 mg drug per gram of nanosorbent. The anti-mycobacterium activity of the INH loaded PCL-MNP was examined against *M-TB* $H_{37}RV$. The MIC of the compound showed inhibition at concentration 6 µg/ml. For studying the in vitro release, the amount of the drug released in the PBS was calculated by spectrophotometry. The compound showed a strong level of activity in vitro: An initial burst release, 6 days sustained release and a negligible release of the drug Observed for 4 weeks.

Acknowledgments

We wish to thank the authority of the Infectious Disease and Tropical Medicine Research Center and Vice Chancellor for Food and Drug , Zahedan University of Medical Sciences and Department of Chemistry, Payame Noor University, Tehran, I.R. of Iran for supporting this work.

Conflict of Interest

The authors declare they have no conflict of interest.

References

1. Venketaraman V, editor. Understanding the host immune response against mycobacterium tuberculosis infection. Springer International Publishing; 2018. doi:10.1007/978-3-319-97367-8
2. Horita Y, Alsultan A, Kwara A, Antwi S, Enimil A, Ortsin A, et al. Evaluation of the adequacy of WHO revised dosages of the first-line antituberculosis drugs in children with tuberculosis using population pharmacokinetic modeling and simulations. Antimicrob Agents Chemother. 2018;62(9):e00008-18. doi:10.1128/AAC.00008-18
3. Ho C-M, Clemens DL, Clemens B-YL, Horwitz MA, Vite AMS, Kee T, et al, Inventors; University of California. Multi-drug therapies for tuberculosis treatment. European Patent Office EP3215225A4. 2018.
4. Dutt M, Khuller GK. Sustained release of isoniazid from a single injectable dose of poly (DL-lactide-co-glycolide) microparticles as a therapeutic approach towards tuberculosis. Int J Antimicrob Agents. 2001;17(2):115-22. doi:10.1016/s0924-8579(00)00330-7
5. Garg T, Rath G, Goyal AK. Inhalable chitosan nanoparticles as antitubercular drug carriers for an effective treatment of tuberculosis. Artif Cells Nanomed Biotechnol. 2016;44(3):997-1001. doi:10.3109/21691401.2015.1008508
6. Saikia C, Hussain A, Ramteke A, Sharma HK, Deb P, Maji TK. Carboxymethyl starch-coated iron oxide magnetic nanoparticles: A potential drug delivery system for isoniazid. Iran Polym J. 2015;24(10):815-28. doi:10.1007/s13726-015-0370-z
7. He H, Lu Y, Qi J, Zhu Q, Chen Z, Wu W. Adapting liposomes for oral drug delivery. Acta Pharm Sin B. 2019;9(1):36-48. doi:10.1016/j.apsb.2018.06.005
8. Varghese S, Anil A, Scaria S, Abraham E. Nanoparticulate technology in the treatment of tuberculosis: A review. Int J Pharm Sci Res. 2018;9(10):4109-16. doi: 10.13040/IJPSR.0975-8232.9(10).4109-16
9. Sang G, Bardajee GR, Mirshokraie A, Didehban K. A thermo/pH/magnetic-responsive nanogel based on sodium alginate by modifying magnetic graphene oxide: Preparation, characterization, and drug delivery. Iran Polym J. 2018;27(3):137-44. doi:10.1007/s13726-017-0592-3
10. El-Boubbou K. Magnetic iron oxide nanoparticles as drug carriers: preparation, conjugation and delivery. Nanomedicine (Lond). 2018;13(8):929-52. doi:10.2217/nnm-2017-0320
11. Sriram K, Maheswari PU, Begum KMMS, Arthanareeswaran G. Functionalized chitosan with super paramagnetic hybrid nanocarrier for targeted drug delivery of curcumin. Iran Polym J. 2018;27(7):469-82. doi:10.1007/s13726-018-0624-7

12. Kadian R. Nanoparticles: A promising drug delivery approach. Asian J Pharm Clin Res. 2018;11(1):30-5. doi:10.22159/ajpcr.2018.v11i1.22035
13. Kamaly N, Yameen B, Wu J, Farokhzad OC. Degradable Controlled-Release Polymers and Polymeric Nanoparticles: Mechanisms of Controlling Drug Release. Chem Rev. 2016;116(4):2602-63. doi:10.1021/acs.chemrev.5b00346
14. Pundir S, Badola A, Sharma D. Sustained release matrix technology and recent advance in matrix drug delivery system: A review. Int J Drug Res Tech. 2017;3(1):12-20.
15. Khodaverdi E, Aboumaashzadeh M, Tekie FSM, Hadizadeh F, Tabassi SAS, Mohajeri SA, et al. Sustained drug release using supramolecular hydrogels composed of cyclodextrin inclusion complexes with pcl/peg multiple block copolymers. Iran. Polym J. 2014;23(9):707-16. doi:10.1007/s13726-014-0265-4
16. Ottenbrite RM, Kim SW. Polymeric Drugs and Drug Delivery Systems. Boca Raton:CRC Press; 2019.
17. Dash TK, Konkimalla VB. Poly-ϵ-caprolactone based formulations for drug delivery and tissue engineering: A review. J Control Release. 2012;158(1):15-33. doi:10.1016/j.jconrel.2011.09.064
18. El Ghandoor H, Zidan H, Khalil MMH, Ismail MIM. Synthesis and some physical properties of magnetite (Fe_3O_4) nanoparticles. Int J Electrochem Sci. 2012;7(6):5734-45.
19. Hosseini M, Haji-Fatahaliha M, Jadidi-Niaragh F, Majidi J, Yousefi M. The use of nanoparticles as a promising therapeutic approach in cancer immunotherapy. Artif Cells Nanomed Biotechnol. 2016;44(4):1051-61. doi:10.3109/21691401.2014.998830
20. Hameed A, Mushtaq HM, Hussain M. Magnetite (fe3o4)-synthesis, functionalization and its application. Int J Food & App Sci. 2017;3(2):64-75. doi:10.21620/ijfaas.2017264-75
21. Gupta AK, Gupta M. Synthesis and surface engineering of iron oxide nanoparticles for biomedical applications. Biomaterials. 2005;26(18):3995-4021. doi:10.1016/j.biomaterials.2004.10.012
22. Mondal J, Sen T, Bhaumik A. Fe3o4@ mesoporous sba-15: A robust and magnetically recoverable catalyst for one-pot synthesis of 3, 4-dihydropyrimidin-2 (1 h)-ones via the biginelli reaction. Dalton Trans. 2012;41(20):6173-81. dio:10.1039/c2dt30106g
23. Hombreiro Pérez M, Zinutti C, Lamprecht A, Ubrich N, Astier A, Hoffman M, et al. The preparation and evaluation of poly(epsilon-caprolactone) microparticles containing both a lipophilic and a hydrophilic drug. J Control Release. 2000;65(3):429-38. doi:10.1016/s0168-3659(99)00253-9
24. Laganas V, Alder J, Silverman JA. In vitro bactericidal activities of daptomycin against S*taphylococcus aureus* and *Enterococcus faecalis* are not mediated by inhibition of lipoteichoic acid biosynthesis. Antimicrob Agents Chemother. 2003;47(8):2682-4. doi:10.1128/aac.47.8.2682-2684.2003
25. Aminoff MJ, Basbaum AI, Benowitz NL, Biaggioni I, Bikle DD, Boushey HA, et al. Katzung BG, editor. Basic & Clinical Pharmacology. 2012. Available at: https://accessmedicine.mhmedical.com/book.aspx?bookID=2249
26. Kajjari PB, Manjeshwar LS, Aminabhavi TM. Novel pH- and temperature-responsive blend hydrogel microspheres of sodium alginate and PNIPAAm-g-GG for controlled release of isoniazid. AAPS PharmSciTech. 2012;13(4):1147-57. doi:10.1208/s12249-012-9838-8
27. Okada H, Doken Y, Ogawa Y, Toguchi H. Preparation of three-month depot injectable microspheres of leuprorelin acetate using biodegradable polymers. Pharm Res. 1994;11(8):1143-7. doi:10.1023/a:1018936815654
28. Pandey R, Zahoor A, Sharma S, Khuller GK. Nanoparticle encapsulated antitubercular drugs as a potential oral drug delivery system against murine tuberculosis. Tuberculosis (Edinb). 2003;83(6):373-8. doi:10.1016/j.tube.2003.07.001
29. Rastogi R, Sultana Y, Aqil M, Ali A, Kumar S, Chuttani K, Mishra AK. Alginate microspheres of isoniazid for oral sustained drug delivery. Int J Pharm. 2007;334(1-2):71-7. doi:10.1016/j.ijpharm.2006.10.024
30. Katzung BG, Masters SB, Trevor A J. 3rd edition. Basic & clinical pharmacology. 2004. Available at: https://accessmedicine.mhmedical.com/content.aspx?bookid=1193&sectionid=66950922
31. Berendsen HJ, Postma Jv, van Gunsteren WF, DiNola A, Haak JR. Molecular dynamics with coupling to an external bath. J Chem Phys. 1984;81(8):3684-90. doi:10.1063/1.448118
32. Parrinello M, Rahman A, Argonne National Laboratory. Polymorphic transitions in single crystals: A new molecular dynamics method. J Appl Phys. 1981;52(12):7182-90. doi:10.1063/1.328693
33. Bagchi T, Chauhan S. Nanotechnology-based approaches for combating tuberculosis: A review. Current Nanomaterials. 2018;3(3):130-9. doi:10.2174/2405461503666181011142949
34. Hess B, Bekker H, Berendsen HJC, Fraaije JGEM. Lincs: A linear constraint solver for molecular simulations. J Comput Chem. 1997;18(12):1463-72. doi:10.1002/(SICI)1096-987X(199709)18:12%3C1463::AID-JCC4%3E3.0.CO;2-H
35. Gunasekaran S, Sailatha E, Seshadri S, Kumaresan S. Ftir, ft raman spectra and molecular structural confirmation of isoniazid. Indian J Pure Appl Phy. 2009;47(1):12-8.